Advanced Physical Research
Vol.8, No.1, 2026, pp.111-129
https://doi.org/10.62476/apr.81101

EVALUATION OF THE RADIOACTIVITY OF RADON GAS AND MEASURING THE RADON CONCENTRATIONS FOR SOME SAMPLES OF IMPORTED AND LOCAL COAL IN KIRKUK CITY

Hanan M. Saleh[1], **Lana H. Mohammed**[1], **Berivan M. Abdullah**[1*], **Ahmed Abed Ibrahim**[2], **Mohammed Ahmed Omar**[3]

[1]College of Education for Women, Department of Physics, University of Kirkuk, Kirkuk, Iraq
[2]Department of Physics, University of Kirkuk, College of Science, Kirkuk, Iraq
[3]Health, Safety and Environment Authorly, North Gas Company, Kirkuk, Iraq

Abstract. This study investigates the radioactivity of radon gas (^{222}Rn) and its exhalation behavior from both imported and local coal samples used in Kirkuk City, Iraq. Coal is known to contain naturally occurring radioactive materials (NORM), including uranium (^{238}U), thorium (^{232}Th), and their decay products, which can pose radiological health risks during storage and combustion. Using CR-39 solid-state nuclear track detectors over a 60-day exposure period, radon concentrations were assessed in coal samples before and after combustion, with both surface (EA) and bulk exhalation rates (EM) rigorously determined. The findings showed that radon concentrations in the air prior to combustion varied from 55 to 80 $Bq \cdot m^{-3}$, suggesting that the main source of indoor radon is raw coal. On the other hand, post-combustion concentrations in coal residues were roughly two orders of magnitude higher, rising sharply to 3800-9300 $Bq \cdot m^{-3}$. After combustion, radon concentrations in the surrounding air ranged from 45 to 100 $Bq \cdot m^{-3}$, within WHO standards but potentially dangerous in poorly ventilated areas. Additionally, compared to pre-combustion values ($2.5 - 3.8\ mBq \cdot m^{-2}h^{-1}$), surface exhalation rates increased after combustion ($1.5 - 4.5\ mBq \cdot m^{-2}h^{-1}$), suggesting greater radon release as a result of structural breakdown and radioactive concentration in ash. Additionally, mass exhalation rates increased dramatically, from $0.2 - 0.7\ mBq \cdot m^{-2}h^{-1}kg^{-1}$ prior to combustion to $0.4 - 2.8\ mBq \cdot m^{-2}h^{-1}kg^{-1}$ following. While the link with mass exhalation rates was limited ($R^2 \approx 0.30$), a strong linear correlation ($R^2 = 1$) was observed between air radon concentration and surface exhalation rates, highlighting the prominent role of surface features in radon emission. In summary, this research emphasizes the substantial increase in radon emission potential from coal combustion, underscoring the need for adequate ventilation, responsible ash management practices, and ongoing radiological monitoring to minimize exposure risks in both professional and domestic environments.

Keywords: Activity concentration, Radionuclide, Coal, Kirkuk City, CR detector.
Corresponding author: Berivan M. Abdullah, University of Kirkuk, College of Education for Women, Department of Physics, Kirkuk, Iraq, e-mail: *berivan-mohammed@uokirkuk.edu.iq*
Received: 12 November 2025; Revised: 12 December 2025; Accepted: 5 January 2026; Published: 18 February 2026.

1 Introduction

Although coal is still a crucial source of energy in the globe, it frequently contains trace levels of naturally occurring radioactive materials (NORM), such as uranium (U) and thorium (Th), as well as the byproducts of their decay, such as radon gas (Rn) and radium (Ra). These radionuclides may accumulate in the surrounding environment during mining, transportation, and coal burning, endangering the public's and employees' radiological health.

The use of coal, both imported and produced in Iraq, has increased in Kirkuk City and other parts of Iraq over the last few years for industrial and household use. But only a few studies have examined the radioactive content of various coal sources. This study seeks to address the deficiency by analyzing radon levels in selected coal samples and evaluating the potential radiological risks associated with their use.

Radon-222 is a naturally occurring radioactive noble gas generated from the decay of uranium-238 in rocks, soils, and raw materials such as coal (UNSCEAR, 2000). Although radon is colorless, odorless, and tasteless, it poses a significant radiological hazard because it emits alpha particles. Long-term exposure to elevated radon levels and their decay products is recognized as the second leading cause of lung cancer worldwide, after smoking (WHO, 2009; Darby et al., 2005).

Coal, whether locally produced or imported, may contain varying concentrations of naturally occurring radionuclides, including uranium, thorium, and potassium-40 (Papastefanou, 2008). Under conditions of combustion or storage in confined spaces, radon can be released into the surrounding environment, thereby increasing radiation exposure to both workers and the public (Oberstedt & Vanmarcke, 1996). Assessing radon activity in coal is therefore essential for evaluating potential health risks and ensuring compliance with international radiation protection standards (ICRP, 2007).

In Iraq, research on natural radioactivity has mostly focused on soils, water, and construction materials rather than coal. ^{226}Ra,^{232}Th, and ^{40}K concentrations were reported in early research on Kirkuk soils, along with hazard indices (Kheder et al., 2025; Taqi et al., 2018). The significance of building materials to indoor radiation exposure was later confirmed by a study conducted in Kirkuk (Wais et al., 2025; Taqi et al., 2018). Radon levels in tap and groundwater were similarly found to be below international standards; however, further monitoring was advised (Munshed & Ibrahim, 2024). The mapping of soil radon in Kirkuk has yielded significant baseline data in recent times (Haws et al., 2024).

A study conducted in Sulaimaniya, in addition to Kirkuk, utilised HPGe detectors to measure ^{226}Ra,^{232}Th, and ^{40}K in coal samples. This study underscored the potential of coal as a natural source of radioactivity (Ahmed, 2022). Additionally, worldwide research has prioritised the exhalation of radon from coal byproducts, including fly ash, which has been associated with environmental exposure (Abdullah, 2025).

Accurate measurement of radon concentrations is commonly achieved using solid-state nuclear track detectors (SSNTDs) such as the CR-39 detector, which provides high sensitivity for detecting alpha particles from radon decay (Kovler et al., 2005). These methods enable estimation of radon exhalation rates and assessment of effective doses to exposed individuals (Nikezic & Yu, 2004).

One of the most popular solid-state nuclear track detectors (SSNTDs) is the CR-39. Cartwright et al. (1978) first used it as a radiation detector in 1978, and because of its high sensitivity and durability, it has since become a vital instrument for identifying charged particles (Topcu et al., 2013). The polymerisation method yields polyallyl diglycol carbonate (PADC), which is used to create the organic polymer detector CR-39. The resulting amorphous hydrocarbon structure is especially well-suited for use in radiation protection, nuclear physics, and environmental radioactivity monitoring due to its exceptional transparency, chemical resistance, and consistent reaction to ionising radiation (Cartwright et al., 1978; Jeong et al., 2017).

This study focuses on coal samples collected from Kirkuk City, Iraq, where both imported and local coal are widely used. The main objectives are to:

1. To measure the concentration of radon gas (^{222}Rn) released from local and imported coal samples used in Kirkuk City.

2. Measure radon concentrations using CR-39 detectors.

3. To compare the levels of natural radioactivity between local and imported coal samples.

Table 1: Sample codes and corresponding weights of coal before and after combustion

Sample Code (Before Combustion)	**Country of origin**	**Weight (gm)**	**Sample Code (After Combustion)**	**Weight (gm)**
CP1	Jordon	8.4	CB1	4.3
CP2	Iraq	5.8	CB2	1.3
CP3	Iraq	8.9	CB3	3.9
CP4	Ireland	6.8	CB4	5.9
CP5	Kuwait	8.0	CB5	7.3
CP6	Indonesia	9.7	CB6	4.6
CP7	china	9.7	CB7	4.4

2 Material and Method

2.1 Sample Collection and Preparation

Two different techniques were used to prepare the coal samples for this investigation. The first approach involved using various sample weights to grind both imported and domestic coal samples into a fine powder, then placing them in the irradiation tube with a consistent sample height of 0.62 cm. In the second technique, the coal samples were burned before measurement, and the ash produced was then placed in the irradiation tube at the same height as the samples (0.62 cm). Because of the various physical and chemical changes that occur throughout the combustion process, it was found that the mass of the combusted samples was less than that of the unburnt coal samples. Carbon makes up the majority of coal, along with variable proportions of moisture, volatile matter, and inorganic minerals. As a result, burning causes loss of water content and volatile components, lowering the samples' total mass.

2.2 Experimental Setup

A. The Irradiation Tube and Detector

The experimental setup used in this study was created especially to measure the amounts of radionuclides emitted from coal samples. Because of its exceptional sensitivity to alpha particles released by radon and its offspring, a 400 μm-thick CR-39 solid-state nuclear track detector was used. Each cylindrical plastic chamber in the irradiation system measured 6.2 cm in length and 3.8 cm in inner diameter, resulting in an effective air column length of 5.58 cm.

Samples of coal, both domestic and foreign, were meticulously prepared and positioned inside the irradiation tubes at a consistent 0.62 cm height. Each chamber had a CR-39 detector installed at the top to guarantee direct exposure to the radon gas released from the coal matrix. Thus, as schematically shown in Figure (1-a) , alpha tracks related to radon isotope decay could be reliably registered.

Figure (1-a)

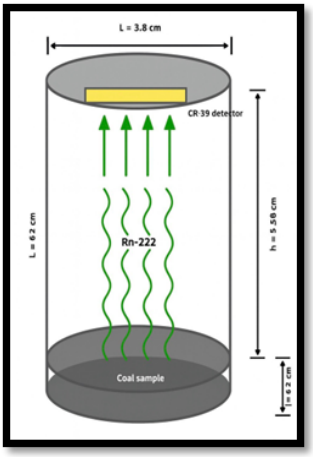

Figure (1-b)

Figure (1-c)

Figure 1: (1-a) : represent the irradiation tube, Figure (1-b) : Prepared coal samples (CP1–CP7) before combustion, placed in sealed plastic containers with proper labeling for subsequent irradiation measurements and Figure (1-c): Coal ash samples (CB1–CB7) after combustion, showing reduced mass and physical changes, stored in labeled containers for irradiation experiments.

B. Etching Solution (NaOH)

Following a 60-day exposure of CR-39 nuclear track detectors (with an effective surface area of $1 \times 1 cm^2$) to radon emitted from coal samples within the irradiation chambers, the detectors were meticulously extracted for chemical etching. The etching procedure involved submerging the detectors in a 6.25 N NaOH aqueous solution and maintaining them in a thermostatically controlled water bath at 70 ± 1 °C for three consecutive hours. After etching, the detectors were meticulously cleaned with distilled water to remove residual alkali and ensure the clarity of the generated tracks.

The latent alpha tracks on the detector surface were disclosed and counted using an optical microscope at maximum magnification (40×), with an initial inspection conducted at a lower magnification (10×), as depicted in Figure 2 (a).

Figure (2-a)

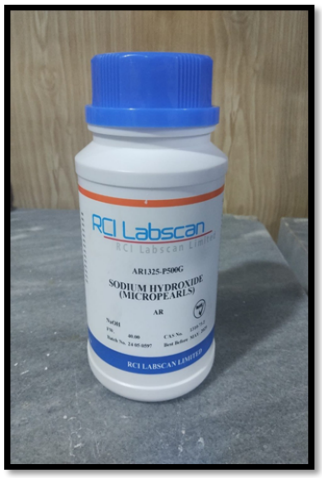

Figure (2-b)

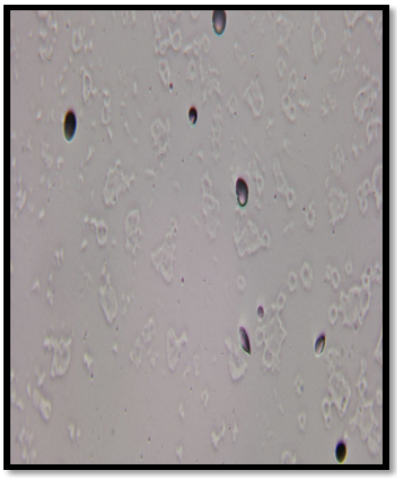

Figure (2-c)

Figure 2: (2-a): represent "Fig. 2A: An optical microscope for visualising and analysing detector traces, with magnifications of 10X and 40X, linked to a digital screen, Figure (2-b): Sodium hydroxide (NaOH) used in CR-39 detector chemical etching and Figure (2-c): A picture of the etched tracks that developed on one of the sample detectors' surfaces.

3 Measurements Procedure

3.1 Radon Concentration

The experimental measurements were conducted using a 400 μm-thick CR-39 solid-state nuclear track detector, which was manufactured in the United Kingdom. Initially, the coal samples (both imported and local) were dried, pulverised, and sieved to ensure that the prepared specimens had a uniform particle size. Each sample was subsequently placed in a specially designed irradiation tube with a known mass, and the tube was meticulously sealed to prevent radon leakage.

This study's diffusion constant (K) was assessed using the geometry of the irradiation tube. The value of K may change depending on the specific design of the irradiation chamber, due to variations in the tube's geometrical parameters, particularly its diameter and length. Consequently, the diffusion constant was ascertained by employing the established relationship (Durrani et al., 2013):

$$K = \frac{1}{4} r \left(2\cos\theta c \ - \frac{r}{R\alpha} \right) \tag{1}$$

The irradiation tube has a radius (r) of 1.9 cm, the detector's critical angle is around (35°), and the range of alpha particles produced by radon in air is ($R\alpha = 4$ cm). Then, after substituting the numbers in the above equation, we see that the diffusion constant K is equal to ($K = 0.552615\ Tr.cm^{-2}d^{-1}/Bq.m^{-3}$).

Subsequently, the radon concentration in the air volume C_{Rn}Can be ascertained using the following equation (Qadr et al., 2025):

$$C_{Rn} = |\frac{\rho}{KT} \tag{2}$$

Where (ρ) signifies the track density of the resultant etched tracks, quantified in $Tr.cm^{-2}$, T denotes the irradiation duration, which in this investigation was roughly 60 days; and K indicates the diffusion constant.

The track density (D), indicative of the intensity rate of the recorded tracks, was calculated using the following relation (Elzain et al., 2018):

$$\mathrm{D} = \frac{\rho}{T} \tag{3}$$

The following relation was used Qadr et al. (2025) to calculate the radon concentration in the coal samples:

$$C_s = \frac{\lambda_{Rn} C_a h t}{L} \tag{4}$$

where C_s, represented in $Bq.m^{-3}$, is the radon concentration in the coal samples. The height of the air gap (about 5.58 cm) between the detector's surface and the coal sample's surface is indicated by the parameter (h). The coal sample's effective thickness (around 0.62 cm) inside the irradiation tube is denoted by (L). With a value of 0.1814 day^{-1}, the decay constant of radon is denoted by the expression (λ_{Rn}).

A_{Rn}, the radioactivity of radon in the coal samples, was then calculated using the following formula (Kheder et al., 2025):

$$A_{Rn} = C_s V \tag{5}$$

where (A_{Rn}) stands for the coal samples' radon radioactivity (Bq) and (V) is the coal sample's effective volume (m^3). The following relation (Azam et al., 1995) was used to determine the sample volume based on the irradiation tube's geometric dimensions:

$$V = \pi r^2 L \tag{6}$$

In this case, (r) is the irradiation tube's inner radius (1.9 cm), and (L) is the coal sample's thickness (0.62 cm) inside the tube.

3.2 Surface emissions and mass emissions rates of radon

The surface exhalation rate (E_A), which was computed using the following relation [25], was used to assess the amount of radon gas released from the coal samples into the surrounding air.

$$E_A = \frac{C\ \lambda\ V}{AT_e} \tag{7}$$

where, E_A is the surface exhalation rate expressed in $Bq.m^{-2}{\cdot}h^{-1}$. The term C represents the integrated exposure to radon gas in $Bq.m^{-3}{\cdot}h^{-1}$, and is found from the relationship (Ghayyib & Ibrahim, 2024):

$$C\ =\ C_a \tag{8}$$

C_a is radon concentration in the air in Bq.m^{-3} units, while T is the exposure time.

In addition, the mass exhalation rate E_M was also determined, as it provides useful information regarding the radon release rate per unit mass of the coal samples. It was evaluated using the following expression (Mohammed et al., 2024; Bahwireth et al., 2025):

$$E_M = \frac{C\ \lambda\ V}{MT_e} \tag{9}$$

where E_M is the mass exhalation rate of radon $Bq.kg^{-1}{\cdot}h^{-1}$, M is the mass of the coal sample (kg), λ is the decay constant of radon, V is the effective volume of the sample (m^3), and T_e is the effective exposure time.

4 Results

4.1 Radon Concentrations in Coal Samples Before and After Combustion

To assess the effect of the combustion process on radon emission from coal. In Table 2, the concentrations of radon gas in the surrounding air are shown for the samples before combustion and for coal combustion ash. The results provide insight into how thermal treatment affects radon release from the coal matrix. Figures 3 and 4 illustrate the measured radon concentrations ($in\ Bq/m^3$) before and after the combustion process, respectively.

Table 2: Radon gas concentration in coal samples before combustion and coal combustion ash.

Sample code of coal	Radon concentration in coal (Bq/m^3)	Sample code of combustion ash	Radon concentration in combustion ash (Bq/m^3)
CP1	6514.27	CB1	9510.83
CP2	6905.13	CB2	6905.13
CP3	6905.13	CB3	4768.45
CP4	6514.27	CB4	9119.98
CP5	7817.12	CB5	6905.13
CP6	7817.12	CB6	6514.27
CP7	5211.42	CB7	3908.56
Mean	6812.06	Mean	6804.62
Range	5211.42-7817.12	Range	3908.56-9510.83

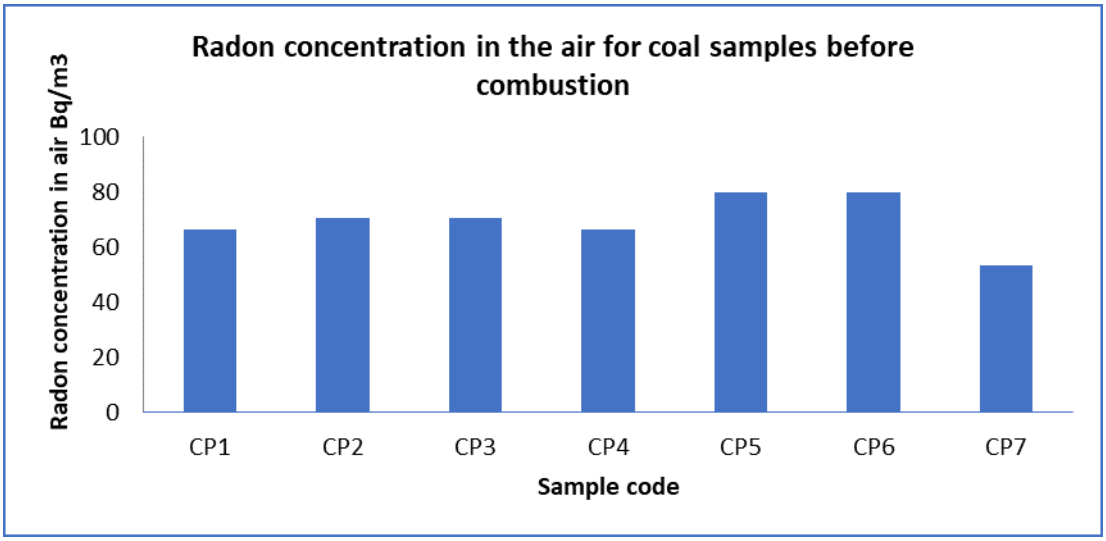

Figure 3: Shows measured radon concentrations in coal samples (CB1–CB7) before the combustion process, expressed in Bq/m^3.

Figure 3 illustrates the radon concentration in air released from coal samples (CP1–CP7) before combustion. The measured concentrations ranged from approximately 55 to 80 Bq·m^{-3}, with noticeable variation among the samples. These results show that radon concentrations in the air of coal samples before combustion ranged between $\approx 58 - 85\ Bq/m^3$, with the highest values recorded in samples CP5 and CP6, and the lowest in CP7. The variations among samples can be attributed to differences in content $\left(^{226}Rn\right)$t as well as physical properties such as porosity and density, which influence the ease of radon release. Although these values are within the internationally accepted indoor air limit (100 Bq/m^3, WHO), they demonstrate that raw coal can serve as a primary source of radon emissions even before combustion, providing a baseline for further comparisons.

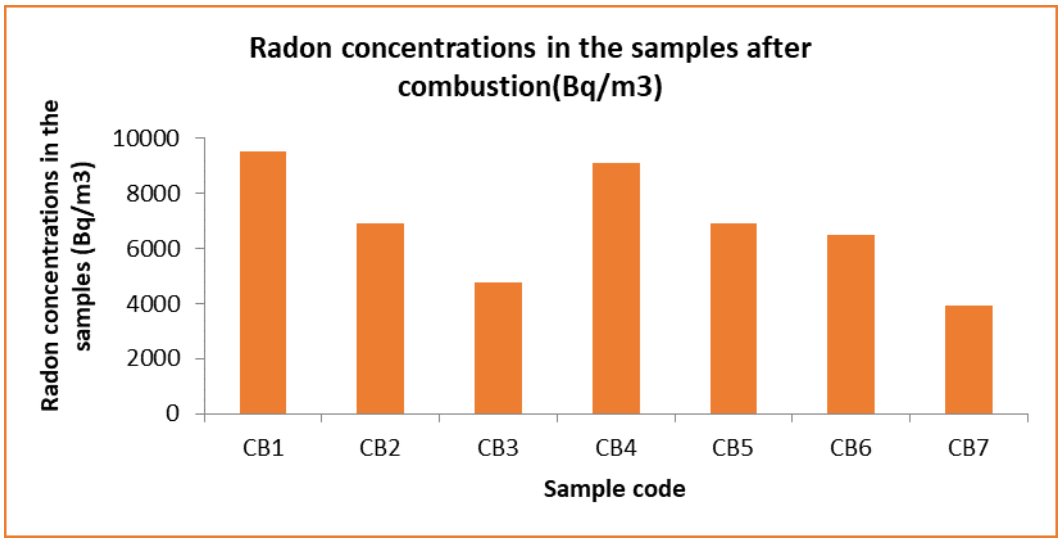

Figure 4: Measured radon concentrations in coal samples (CB1–CB7) following the combustion process, expressed in Bq/m^3.

The figure 4 shows that radon concentrations within coal samples after combustion ranged between $3800 - 9300\ Bq/m^3$, with the highest values observed in samples CB1 and CB4, while the lowest was recorded in CB7. These elevated levels reflect the effect of combustion, which leads to the breakdown of the coal's internal structure and enhances the release of(^{226}Rn) and its

progeny, resulting in greater radon accumulation in the residues. The variation among samples is attributed to differences in mineral composition and physical properties such as density and porosity. These findings confirm that coal combustion not only increases radon emission into the air but also leaves behind high concentrations in coal residues, emphasizing the need for proper ash and waste management to minimize potential radiological risks.

4.2 Radon Concentrations in the Surrounding Air

In addition to measuring radon in the coal itself, the radon concentration in the air surrounding the coal samples was also measured to evaluate dispersion and potential exposure risk. Measurements were performed both before and after combustion for all samples. The obtained results are presented in Figures (5 and 6), which demonstrate the variations in radon concentration in the surrounding air and allow for direct comparison between pre- and post-combustion conditions.

Table 3: Radon gas concentration in the Surrounding air before combustion and coal combustion ash.

Sample code of coal	Radon concentration in air (Bq/m^3)	Sample code of combustion ash	Radon concentration in air (Bq/m^3)
CP1	66.50199506	CB1	97.09291279
CP2	70.49211476	CB2	70.49211476
CP3	70.49211476	CB3	48.67946038
CP4	66.50199506	CB4	93.10279308
CP5	79.80239407	CB5	70.49211476
CP6	79.80239407	CB6	66.50199506
CP7	53.20159605	CB7	39.90119704

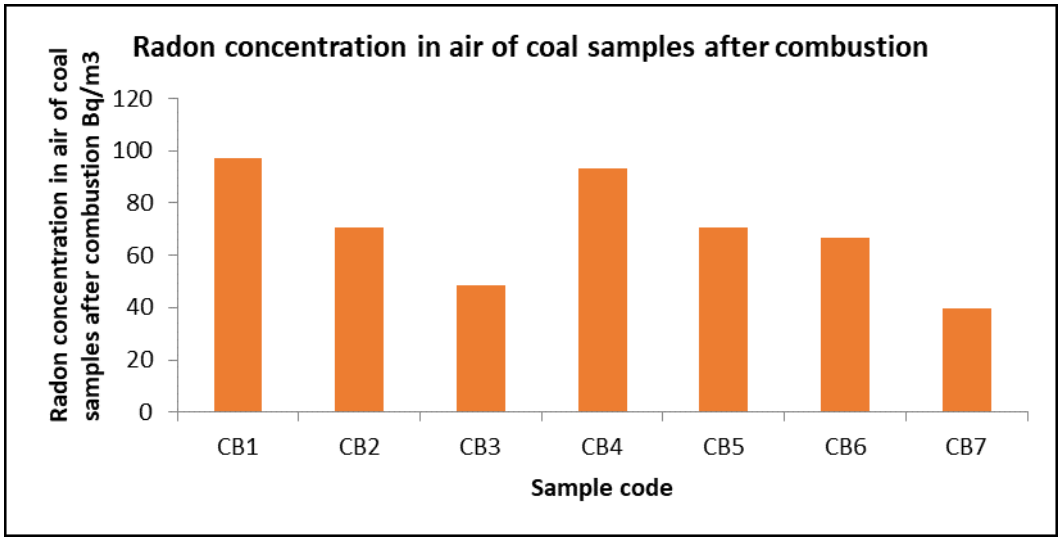

Figure 5: Shows Radon concentration in the air surrounding coal samples (CB1–CB7) after combustion, expressed in Bq/m^3.

In figure 5, Radon concentrations in air after coal combustion ranged between 45–100 Bq/m^3, highest in CB1 and CB4 and lowest in CB7. The increase is linked to coal structure breakdown releasing trapped radon, with variations due to ^{226}Ra content and physical properties. Although within the WHO limit, these values indicate a potential risk in poorly ventilated areas.

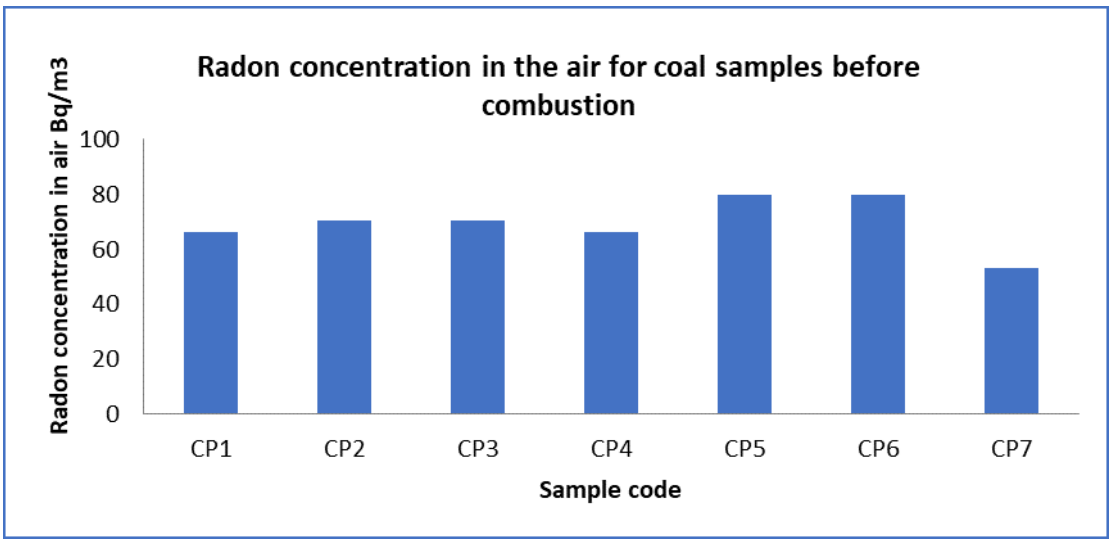

Figure 6: Shows Radon concentration in the air for coal samples before combustion (Bq/m^3).

Figure 6 illustrates the radon concentration in the air surrounding the coal samples before combustion, with values ranging between 40–80 Bq/m^3 depending on the sample (CP1–CP7). These results show relatively close concentrations, which indicates that the initial release of radon from unburned coal mainly depends on:

1. Radium-226 content in the sample: Since ^{226}Ra is the parent nuclide of ^{222}Rn, the variations in radon concentrations reflect differences in the radium content of each coal type.
2. Physical properties of coal (porosity and density): More porous coal samples allow higher radon diffusion into the surrounding air, while denser samples tend to retain the gas.
3. Experimental conditions (exposure time and air volume): The volume of air inside the irradiation tube and the exposure duration directly affect the measured radon concentrations.

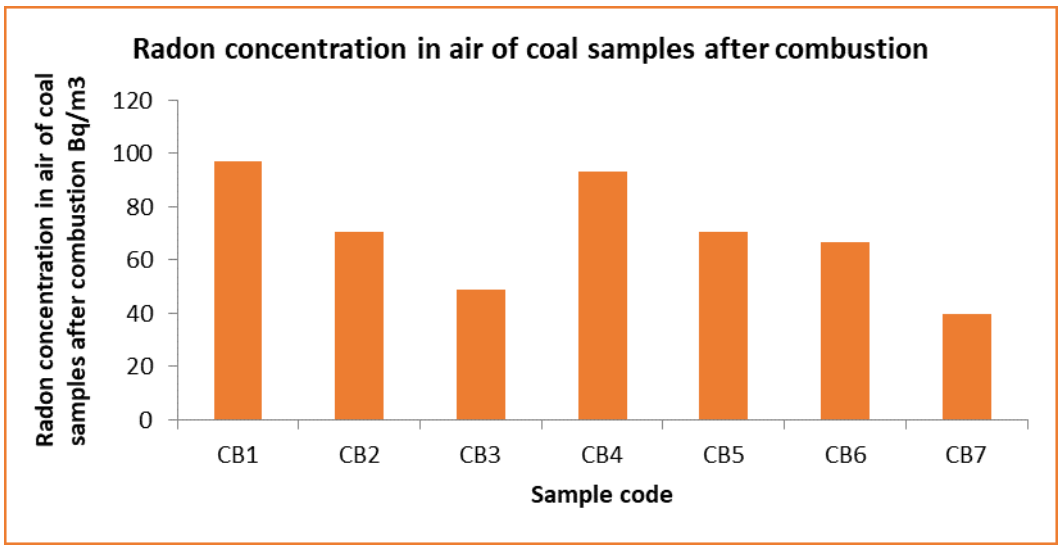

Figure 7: Shows Radon concentration in the air of coal samples after combustion (Bq/m^3).

Figure 7 presents the radon concentration in the air of coal samples after combustion, with values ranging between $20 - 100$ Bq/m^3. The highest concentrations were observed in samples CB1 and CB4 (close to $90 - 100$ Bq/m^3), whereas lower values were recorded for CB6 and CB7 (below 40 Bq/m^3).

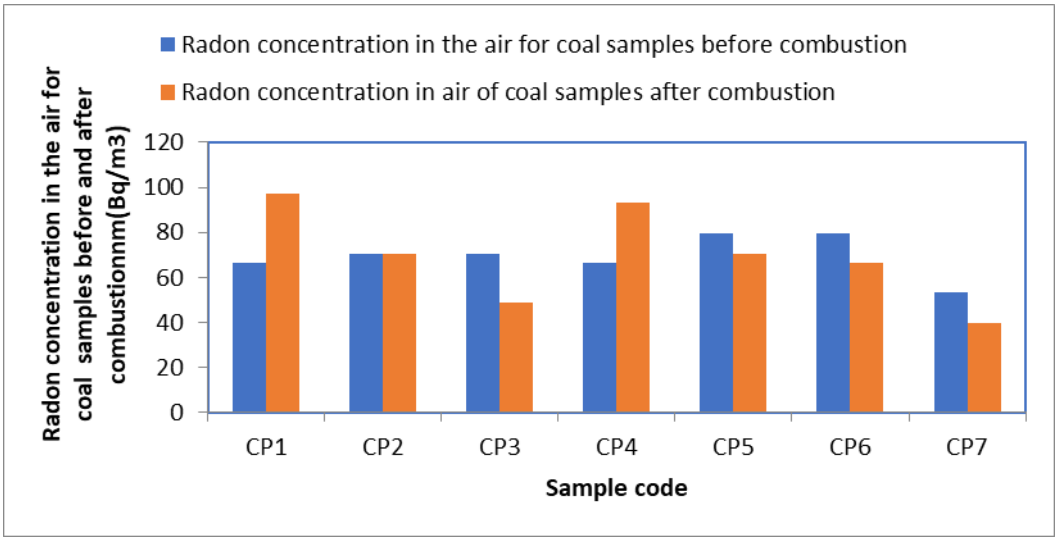

Figure 8: Shows Comparison of radon concentration in the air of coal samples before and after combustion (Bq/m^3).

As demonstrated in Figure 8, radon concentrations in all coal samples exhibited an increase following combustion relative to their pre-combustion levels. The increase varied from 10 to 30 Bq/m^3 across samples CP1–CP7. The most significant increase was observed in CP1 and CP4, where radon concentrations neared 100 Bq/m^3 following combustion, compared to approximately $70-80$ Bq/m^3 prior to burning. This phenomenon can be attributed to the disintegration of the coal's structure during combustion, which facilitates radon release by liberating radon generated from the decomposition of radium-226 previously confined within the solid coal matrix.

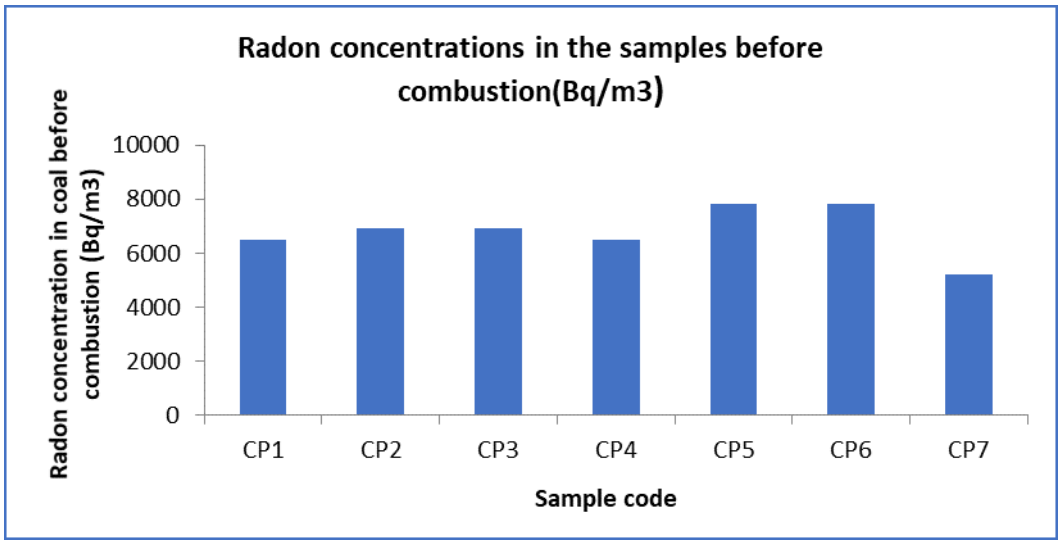

Figure 9: Shows Radon concentrations in the air of coal samples before combustion (Bq/m^3).

As illustrated in Figure 9, all coal samples demonstrated elevated radon concentrations following combustion, with increases ranging from 10 *to* 30 Bq/m^3. Samples CP1 and CP4 exhibited the highest measurements, nearing 100 Bq/m^3. This behavior can be ascribed to changes in the internal structure of the coal during combustion, which facilitates the release of radon previously confined within fissures and mineral matrices. The observed variations among the samples are probably associated with differences in ^{226}Ra content, mineral composition, and physical characteristics of the coal. These findings emphasize combustion as a principal process affecting radon exhalation and underscore its significance in evaluating environmental

and radiological health implications.

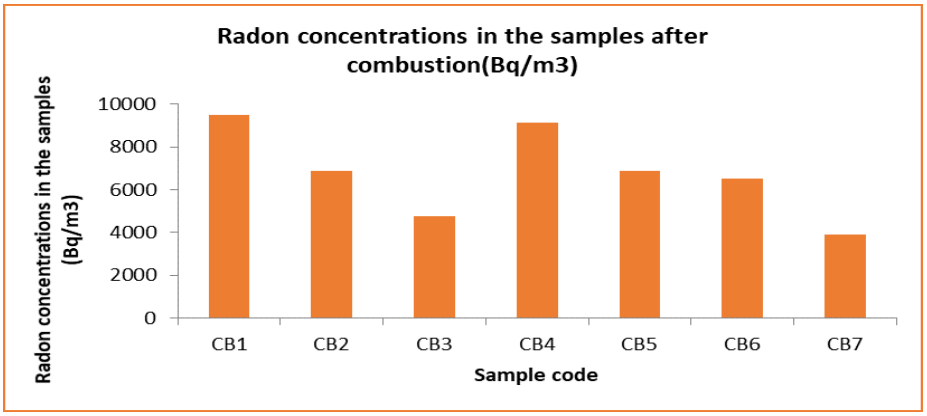

Figure 10: Shows Radon concentrations in the air of coal samples after combustion (Bq/m^3).

As illustrated in Figure 10, the post-combustion coal samples had radon concentrations that ranged from roughly 2000 to 9000 Bq/m^3, with samples CB1 and CB4 having the highest values. A significant amount of radon may still be trapped in the ash and residual coal structure after combustion, as indicated by the significant discrepancy between the radon levels inside the samples and those found in the air. In addition to the ash's high porosity, which improves gas retention, this behavior is primarily explained by the buildup of radium-226 and its decay products in the leftover material. Variability between samples is attributed to variations in the coal's physical properties, mineral makeup, and radium concentration.

4.3 Surface Exhalation Rates (EA) of Radon

The radon surface exhalation rate (EA) reflects the amount of radon emitted per unit area of coal into the surrounding air and serves as a key parameter in assessing the radiological impact of coal usage. Figures 11 and 12 show that the EA values measured before and after combustion show a clear rise after burning. This means that combustion greatly increases the amount of radon that comes out of the coal surface. This behavior shows how thermal alteration can change the physical structure of coal and make it easier for radon to escape.

In the table 4 the surface exhalation rate (EA) of radon from coal samples represents the rate at which radon escapes through the coal surface into the atmosphere. This parameter is crucial for estimating the contribution of coal to indoor or ambient radon levels. Figures 11 and 12 display the measured EA values ($mBq \cdot m^{-2} \cdot h^{-1}$) for all samples before and after combustion, respectively, showing the effect of burning on the surface release behavior of radon.

Table 4: The surface exhalation rate (EA) of radon for coal samples and coal combustion ash

Sample code of coal	(EA) Radon ($mBq \cdot m^{-2} \cdot h^{-1}$)	Sample code of coal combustion ash	(EA) Radon coal combustion ash ($mBq \cdot m^{-2} \cdot h^{-1}$)
CP1	3.09	CB1	4.51
CP2	3.28	CB2	3.28
CP3	3.28	CB3	2.26
CP4	3.09	CB4	4.33
CP5	3.71	CB5	3.28
CP6	3.71	CB6	3.09
CP7	2.47	CB7	1.86
Mean	3.23	Mean	3.23
Range	2.47-3.71	Range	1.86-4.51

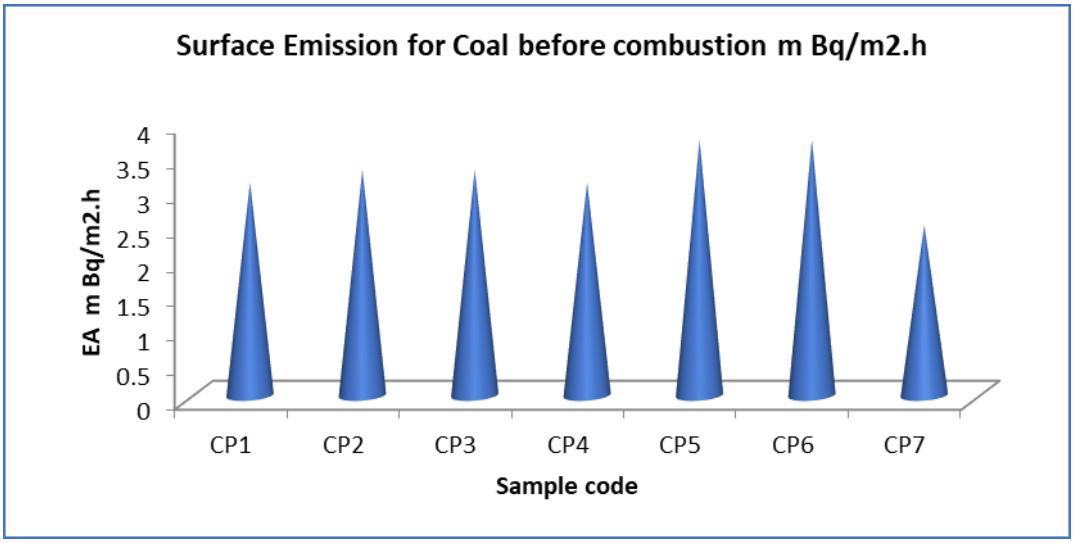

Figure 11: Shows Surface exhalation rate (E_A) of radon from coal samples (CP1–CP7) before combustion, expressed in $mBq \cdot m^{-2} \cdot h^{-1}$

Figure 11 illustrates the surface exhalation rate (E_A) of ^{222}Rn from coal samples before combustion. The obtained values ranged between 2.5 *and* 3.8 $mBq \cdot m^{-2} \cdot h^{-1}$, reflecting a clear variation among the investigated samples (CP1–CP7). The highest exhalation rates were recorded in samples CP5 and CP6 (approaching 3.8 ($mBq \cdot m^{-2} \cdot h^{-1}$), which may be attributed to relatively higher concentrations of uranium-238 and its decay products. In contrast, sample CP7 exhibited the lowest E_A value (around 2.5 $mBq \cdot m^{-2} \cdot h^{-1}$), most likely due to a lower content of ^{226}Ra or differences in physical–chemical characteristics such as porosity and density.

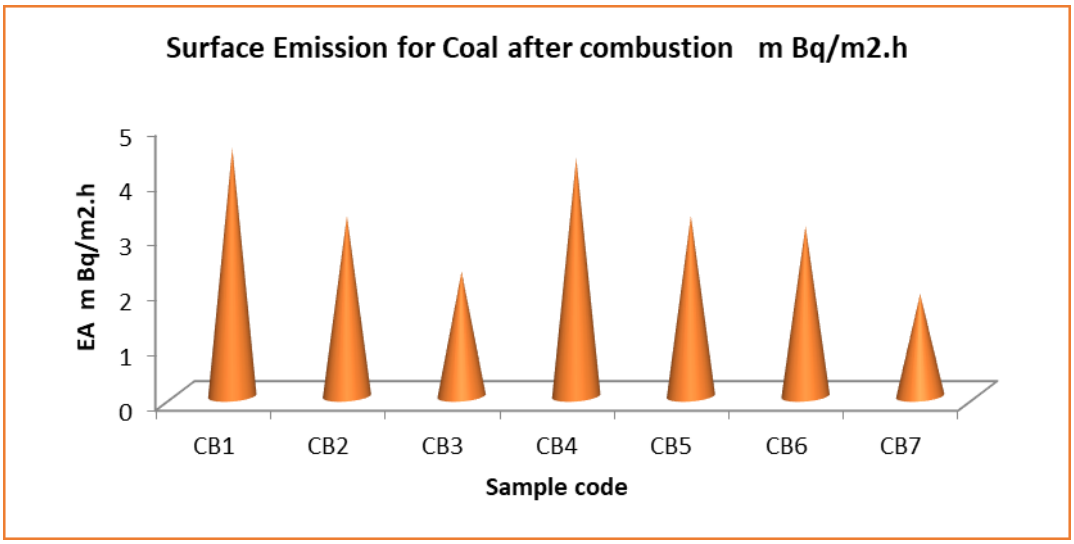

Figure 12: Shows Surface exhalation rate of radon from coal samples (CB1–CB7) after combustion, expressed in $mBq \cdot m^{-2} \cdot h^{-1}$.

Figure 12 demonstrates that the surface exhalation rate of ^{222}Rn from combusted coal samples varies from 1.5 *to* 4.5 $mBq \cdot m^{-2} \cdot h^{-1}$. Samples CB1, CB4, and CB2 had the highest exhalation values, indicating augmented radon emission correlated with elevated porosity and increased uranium concentration post-combustion. In contrast, diminished values observed for CB3, CB6, and CB7 indicate fluctuations in the mineral composition and physical characteristics of the coal. The overall rise in exhalation rates post-combustion can be ascribed to the concentration of radioactive elements in the residual ash and the structural alterations caused

by thermal treatment. The findings highlight that coal combustion markedly enhances radon emissions, thus heightening radiological exposure concerns, especially in inadequately ventilated indoor settings.

4.4 Mass Exhalation Rates (EM) of Radon

The mass exhalation rate (EM) indicates the radon activity emitted per unit mass of coal and offers more understanding of radon emanation properties beyond surface measurements. Figures 13 and 14 demonstrate that electromagnetic (EM) values measured prior to and subsequent to combustion exhibit a large rise post-burning, indicating the substantial effect of combustion on radon emission. This phenomenon can be ascribed to the accumulation of radioactive materials and structural alterations in the coal matrix post-combustion, which facilitate radon transport and emission.

Table 5: Mass Exhalation Rates (EM) of Radon for coal sample before and after combustion

Sample code of coal	(EM) Radon ($mBq \cdot m^{-2} \cdot h^{-1}kg^{-1}$)	Sample code of coal combustion ash	(EM) Radon coal combustion ash ($mBq \cdot m^{-2} \cdot h^{-1}kg^{-1}$)
CP1	0.42	CB1	1.19
CP2	0.64	CB2	2.86
CP3	0.42	CB3	0.66
CP4	0.52	CB4	0.83
CP5	0.53	CB5	0.51
CP6	0.43	CB6	0.76
CP7	0.29	CB7	0.48
Mean	0.46	Mean	1.04
Range	0.29-0.64	Range	0.48-2.86

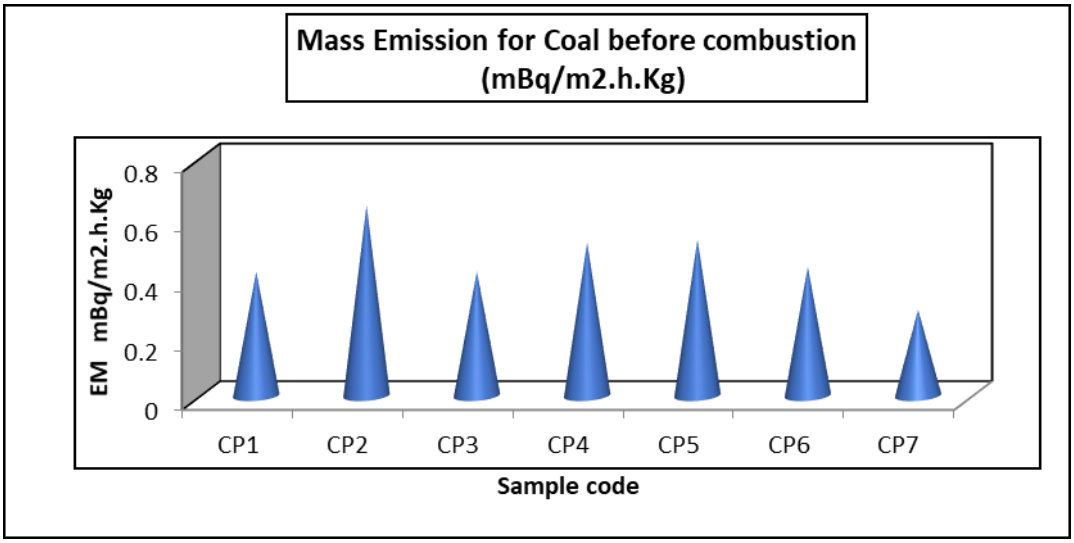

Figure 13: Shows Measured Mass Exhalation Rate (EM) of Radon-222 from Coal Samples (CP1–CP7) Prior to Combustion, Expressed in $mBq \cdot m^{-2} \cdot h^{-1}kg^{-1}$

Figure 13 shows the mass exhalation rate (EM) of ^{222}Rn from coal samples (CP1-CP7) before combustion, with values ranging from about 0.2 to 0.7 $mBq \cdot m^{-2} \cdot h^{-1}kg^{-1}$. Sample CP2 recorded the highest EM value, indicating a higher radium-226 content and greater radon release per unit mass. Moderate values were observed for CP4 and CP5, while lower rates were recorded for CP1, CP6, and CP7.

These results indicate that radon exhalation varies among coal samples depending on their radionuclide content and physical properties. The observed differences highlight the importance

of considering mass-based exhalation rates, alongside surface measurements, to achieve a more accurate assessment of the radiological impact of coal.

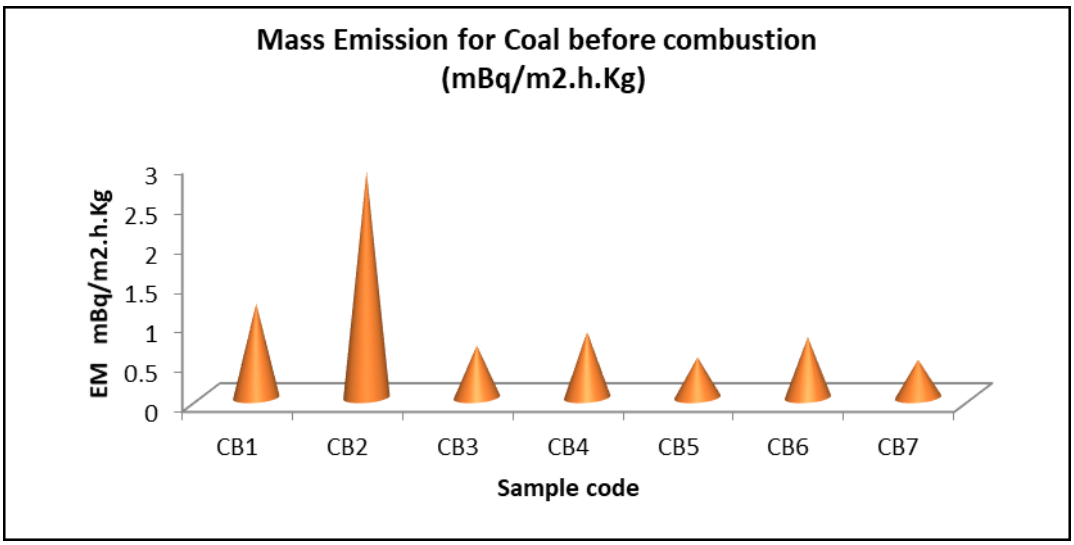

Figure 14: Shows Measured Mass Exhalation Rate (EM) of ^{222}Rn from Coal Samples (CB1–CB7) Following Combustion, Expressed $mBq \cdot m^{-2} \cdot h^{-1}kg^{-1}$

Figure 14 presents the mass exhalation rate (EM) of ^{222}Rn from coal samples after combustion. The values ranged approximately between 0.4 *and* 2.8 $mBq \cdot m^{-2} \cdot h^{-1}kg^{-1}$, showing significant variability among the samples.

Figures 13 and 14 present the mass exhalation rate (EM) of $^{222}Rn$from coal samples before and after combustion, respectively. Before combustion (Figure 8), EM values ranged between 0.2 *and* 0.7 $mBq \cdot m^{-2} \cdot h^{-1}kg^{-1}$, with the highest value observed in sample CP2 ($\sim 0.7\ mBq \cdot m^{-2} \cdot h^{-1}kg^{-1}$). In contrast, after combustion (Figure 9), EM values significantly increased, ranging between 0.4 *and* 2.8 $mBq \cdot m^{-2} \cdot h^{-1}kg^{-1}$, with sample CB2 showing the highest value ($\sim 2.8\ mBq \cdot m^{-2} \cdot h^{-1}kg^{-1}$).

The observed rise in EM values post-combustion can be attributed to the reduction in coal mass during incineration, leading to the concentration of radionuclides-specifically radium-226-in the residual ash. As a result, the leftover material demonstrates an elevated radon emission potential per unit mass relative to unburned coal.

The comparison indicates that combustion significantly increases the mass-based radon exhalation rate. This signifies that coal presents a heightened radiological risk post-combustion, particularly concerning the management and disposal of ash in confined or inadequately ventilated spaces where radon concentration could pose health hazards.

4.5 Correlation and Linear Relationships

Analyses of correlation and linear regression were used to examine the connection between surface and mass exhalation rates and airborne radon levels. This method sheds light on the extent to which radon concentration and its exhalation behavior are correlated. Figures 15 and 16 show the appropriate trends and linear fits for every coal sample.

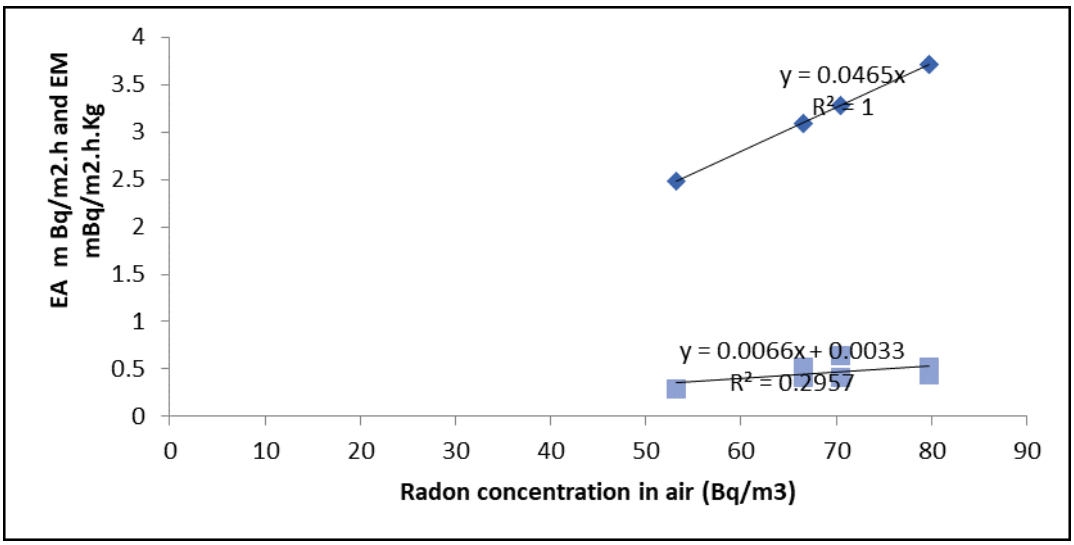

Figure 15: Represents Correlation between radon concentration in air (Bq/m^3) and both surface exhalation rate ($EA,\ mBq \cdot m^{-2} \cdot h^{-1}$) and mass exhalation rate ($EM,\ mBq \cdot m^{-2} \cdot h^{-1} kg^{-1}$) of coal samples

Radon concentration in the air and surface exhalation rate are strongly positively correlated, as Figure 15 illustrates, with value that ($R^2 \approx 1$). This suggests that surface exhalation mechanisms directly affect the amount of radon present. On the other hand, radon concentration and mass exhalation rate have a relatively modest association ($R^2 \approx 0.296$), suggesting that sample mass has less of an impact on radon emission than surface features.

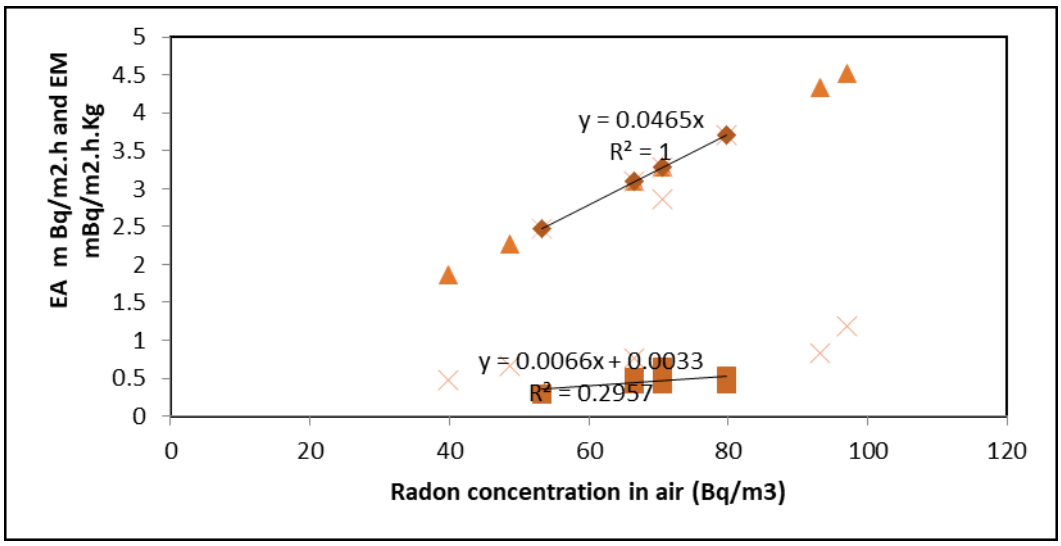

Figure 16: Shows Linear Relationship between Radon Concentration in Air and the Surface (EA) and Mass (EM) Exhalation Rates of Radon from Coal Samples.

The correlation between surface (EA) and mass (EM) exhalation rates and radon concentration in the air is depicted in Figure 16. EA showed a high linear connection with radon concentration (y = 0.0465x, with a correlation coefficient of $R^2 = 1.0$), suggesting a direct proportionate rise. On the other hand, EM showed a minor association ($y = 0.0066x + 0.0033,\ R^2 = 0.2957$), indicating that changes in coal characteristics have a greater impact on mass-based exhalation.

Following combustion, the surface exhalation rate (EA) of ^{222}Rn rose in comparison to pre-combustion values. EA varied between 2.5 *and* 3.8 $mBq \cdot m^{-2} \cdot h^{-1}$ prior to combustion and between 1.5 *and* 4.5 $mBq \cdot m^{-2} \cdot h^{-1}$ following combustion, with sample CB1 showing the

highest value. This rise suggests that, especially in interior settings, combustion increases radon release, raising the possible radiological risk.

4.6 Radon Activity in Coal Samples

The total radon activity was assessed to evaluate the comprehensive radiological effect of coal prior to and following burning. Figures 17 and 18 depict the associated activity values and the impact of combustion on radon concentrations.

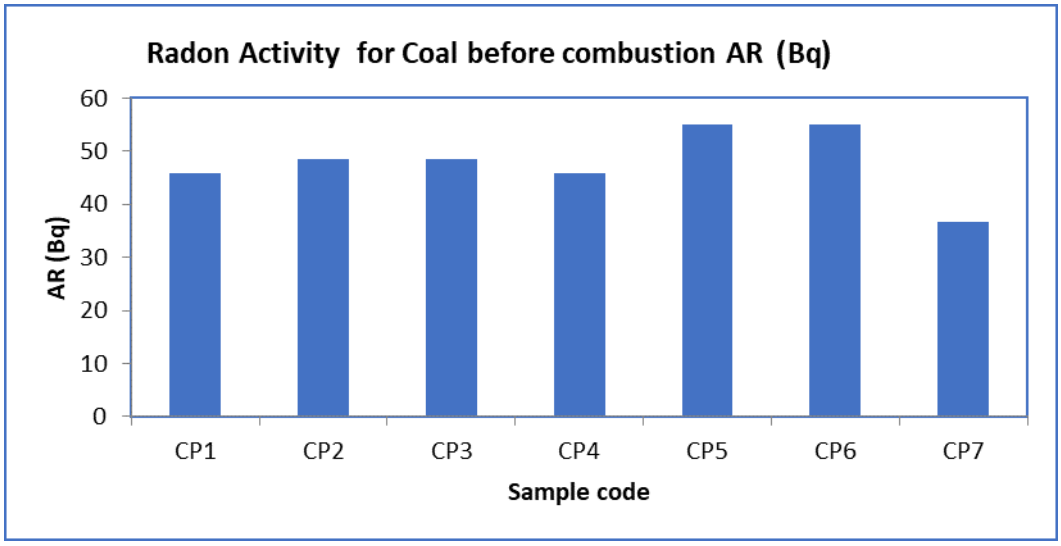

Figure 17: Represent Radon activity in coal samples before combustion (Bq).

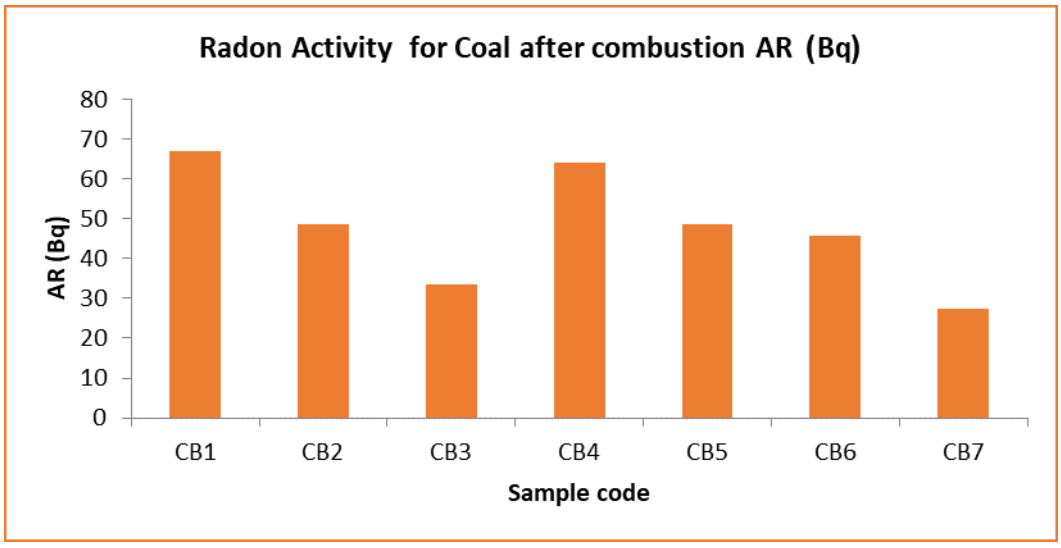

Figure 18: Represent Radon activity in coal samples after combustion (Bq).

Radon activity in coal samples rose after burning, rising from 20–50 Bq before to 20–70 Bq after, as seen in Figures 17 and 18. This rise is explained by the coal matrix's disintegration during burning, which makes it easier for radium and its breakdown products to be released. Variations between samples are linked to variations in the physical characteristics and mineral content, confirming that burning significantly raises radon activity and the accompanying radiological risk.

4.7 Statical Analysis

Radon concentrations before and after combustion were compared using descriptive statistics and Welch's t-test. Coal samples had an average radon concentration of 69.54 ± 9.11 Bq/m^3, while combustion ash had an average of 69.47 ± 20.97 Bq/m^3. There was no statistically significant difference between the two groups (p = 0.993). However, the increased variability in radon levels following combustion is indicated by the higher standard deviation seen in ash samples, indicating that burning influences the distribution of radon rather than its average concentration.

5 Discussion

The findings suggest that radon concentration is significantly influenced by coal type and the combustion process. Prior to combustion, radon concentrations ($55 - 80\ Bq \cdot m^3$) were maintained below the thresholds established by the World Health Organization and the International Commission on Radiological Protection. Conversely, following combustion, a significant increase was observed, with levels reaching $3 \times 10^3 - 9 \times 10^3\ Bq \cdot m^{-3}$, and sample CB1 exhibiting the highest values. The observed increase is primarily attributable to alterations in coal's structural composition, augmented surface area, and the concentration of radionuclides, specifically ^{226}Ra, within the ash.

Additionally, the rate of radon release exhibited a stronger correlation with surface exhalation rate compared to mass exhalation rate, suggesting that surface properties significantly influence radon emanation. The increased emission rates detected following combustion underscore the potential radiological hazard associated with coal ash, particularly within enclosed spaces, thereby necessitating meticulous management and surveillance of combustion byproducts.

6 Conclusions

This investigation indicates that the combustion of coal substantially elevates radon emission levels, with subsequent concentrations surpassing those of unprocessed coal by more than two orders of magnitude. This escalation is predominantly ascribed to structural modifications and the augmentation of ^{226}Ra within the residual ash. While radon emissions from unprocessed coal are comparatively minimal, the combustion process significantly elevates surface exhalation rates, suggesting that coal ash presents a potential radiological hazard. Consequently, appropriate management, storage, and ventilation are imperative to mitigate radiological risks, especially within interior and workplace settings.

References

Abdullah, K.O. Natural radioactivity and dose assessment in coal samples collected from Sulaymaniyah city in Iraqi Kurdistan region. *Acta Geophys.,* 73, 3425–3430 https://doi.org/10.1007/s11600-025-01593-7

Ahmed, R.S. (2022). The concentration of radioactive materials in Iraqi soils, water and plants: A review. *Journal of Radiation Research and Applied Sciences, 15*(1), 245-256. https://doi.org/10.1016/j.jrras.2022.03.012

Ali, M.J., Kheder, M.H., & Azeez, H.N. (2025). Utilizing the CR-39 detector to measure the concentrations of alpha emitters in fish samples from the Nineveh Governorate in Iraq. *The European Physical Journal Plus, 140*(6), 498. https://doi.org/10.1140/epjp/s13360-025-06441-7

Azam, A., Naqvi, A.H., & Srivastava, D.S. (1995). Radium concentration and radon exhalation measurements using LR-115 type II plastic track detectors. *Nuclear geophysics, 9*(6), 653-657.

Bahwireth, M A., AS-Subaihi, F.A., & Bazohair, A.O. (2025). Measurement of Radon Gas Concentration and Radon Exhalation Rate in Cement Samples by using Nuclear Track Detector (CR-39). *ARID International Journal for Science and Technology.* https://doi.org/10.36772/arid.aijst.2025.8156

Cartwright, B.G., Shirk, E.K., & Price, P.B. (1978). A nuclear-track-recording polymer of unique sensitivity and resolution. *Nuclear Instruments and Methods, 153*(2-3), 457-460.

d Technology. (2025) https://doi.org/10.36772/arid.aijst.2025.8156

Darby, S., Hill, D., Auvinen, A., Barros-Dios, J.M., Baysson, H., Bochicchio, F., ... & Doll, R. (2005). Radon in homes and risk of lung cancer: collaborative analysis of individual data from 13 European case-control studies. *BMJ, 330*(7485), 223. https://doi.org/10.1136/bmj.38308.477650.63.

Durrani, S.A., Bull, R.K. (2013). *Solid state nuclear track detection: Principles, Methods And Applications* (Vol. 111). Elsevier.

Elzain, A.E.A. (2018). Indoor radon concentrations in Al-Hasahisa and Rufaa towns in the central part of Sudan. *Scientific Publications of the State University of Novi Pazar Series A: Applied Mathematics, Informatics and mechanics, 10*(2), 87-98. https://doi.org/10.5937/SPSUNP1802087E

Ghayyib, G., Ibrahim, A.A. (2024). Determination the natural radiation activity in female human urine samples in Kirkuk city by using two technique Rad7 and CR-39 detector. *International Journal of Medical Sciences, 7*(1), 18-31.

Haws, J.N., Ibrahim, A.A., & Ibrahim Al-Tamimi, O.S. (2024). Radon concentrations in the Groundwater of Kirkuk city/Iraq. *Kirkuk Journal of Science, 19*(2). https://doi.org/10.32894/kujss.2024.145296.1129

ICRP. International Commission on Radiological Protection. The 2007 Recommendations of the International Commission on Radiological Protection,(ICRP Publication 103. Ann. ICRP 37 (2–4), 2007).

Jeong, T.W., Singh, P.K., Scullion, C., Ahmed, H., Hadjisolomou, P., Jeon, C., ... & Ter-Avetisyan, S. (2017). CR-39 track detector for multi-MeV ion spectroscopy. *Scientific Reports, 7*(1), 2152. https://doi.org/10.1038/s41598-017-02331-w

Kheder, M.H., Azeez, H.N., Kassim, & Basheer, R.A. (2025). Concentrations of alpha emitters in foodstuffs manufactured in the Bashiqa Region in Iraq using CR-39 detector. *Eur. Phys. J. Plus,* 140, 133 https://doi.org/10.1140/epjp/s13360-025-06077-7

Kheder, M.H., Azeez, H.N., Kassim, Y.Y., & Basheer, R.A. (2025). Concentrations of alpha emitters in foodstuffs manufactured in the Bashiqa Region in Iraq using CR-39 detector. *The European Physical Journal Plus, 140*(2), 1-5. https://doi.org/10.1140/epjp/s13360-025-06077-7

Kovler, K., Perevalov, A., Steiner, V., & Metzger, L.A. (2005). Radon exhalation of cementitious materials made with coal fly ash: Part 1–scientific background and testing of the cement and fly ash emanation. *Journal of Environmental Radioactivity, 82*(3), 321-334. https://doi.org/10.1016/j.jenvrad.2005.02.004

Munshed, A.S., Ibrahim, A.A. (2024). The Effect of Two Etching Solutions NaOH and KOH on Registration Properties and Etching of Polymer CR-39 Detectors. *Engineering Chemistry*, 6, 1-9. https://doi.org/10.4028/p-CzNM6C.

Mohammed, L.H., Ibrahim, A.A., & Omer, M.A. (2024). Measurement of Radon Concentrations in Gypsum Stone from Quarries in Northern Iraq Using CR-39 Detector. *International Journal of Recent Research and Review, 17*(4), 1–6

Nikezic, D., Yu, K.N. (2004). Formation and growth of tracks in nuclear track materials. *Materials Science and Engineering: R: Reports, 46*(3-5), 51-123. https://doi.org/10.1016/j.mser.2004.07.003

Oberstedt, S., Vanmarcke, H. (1996). A Radon Exhalation Monitor. *Radiation Protection Dosimetry, 63*(1), 69–72 https://doi.org/10.1093/oxfordjournals.rpd.a031514

Papastefanou, C. (2008). Radioactivity of coals and fly ashes. *J. Radioanal. Nucl. Chem.*, 275, 29–35 https://doi.org/10.1007/s10967-006-6966-1

Qadr, H.M., Salih, N.F., & Hamad, A.M. (2025). Alpha emitter concentrations of natural radionuclides and radiological hazard assessment of soil samples in the Halabja governorate, Iraq. *Isotopes in Environmental and Health Studies*, 1–11. https://doi.org/10.1080/10256016.2025.2550449

Taqi, A.H., Shaker, A.M., & Battawy, A.A. (2018). Natural radioactivity assessment in soil samples from Kirkuk city of Iraq using HPGe detector. *International Journal of Radiation Research, 16*(4), 455-463.

Taqi, A.H., Shaker, A.M., & Battawy, A.A. (2018). Natural radioactivity in building materials from Kirkuk city of Iraq. *J. Rad. Nucl. Appl., 3*(3), https://doi.org/10.18576/jrna/030310.

Topcu, N., Biçak, D., Cam, S., & Erees, F.S. (2013). Radon exhalation rate from building materials using CR-39 nuclear track detector. *Indoor and Built Environment, 22*(2), 384-387. https://doi.org/10.1177/1420326X11426890.

UNSCEAR. United Nations Scientific Committee on the Effects of Atomic Radiation. Sources and effects of ionizing radiation,(UNSCEAR 2000 Report. New York: United Nations, 2000).

Wais, T.Y., Namq, B.F., Najam, L.A., Sayyed, M.I., Najemalden, M.A., Ahmed, R.T., ... & Mansour, H. (2025). Measurement of radon activity concentration, estimating the annual effective dose, and the lifetime cancer risk in the soil of Kirkuk Province, Northern Iraq, using AlphaGUARD. *The European Physical Journal plus, 140*(7), 707. https://doi.org/10.1140/epjp/s13360-025-06642-0

WHO. World Health Organization. Handbook on indoor radon: a public health perspective (Geneva: WHO Press, 2009).